Electronic Supplementary Information (ESI)

Hydrogen-Induced Structural Transformation of AuCu Nanoalloys Probed by Synchrotron X-ray Diffraction Techniques

M. Yamauchi,*[a,b] K. Okubo,[a,b] T. Tsukuda,[c,d] K. Kato,*[b,e] M. Takata,[e] and S. Takeda[f]

[a]WPI-I2CNER, Kyushu University, Motooka 744, Nishi-ku, Fukuoka 819-0395, Japan

[b]CREST, JST, 4-1-8 Honcho, Kawaguchi, Saitama 332-0012, Japan

[c]Department of Chemistry, School of Science, The University of Tokyo, Hongo 7-3-1, Bunkyo-ku, Tokyo 113-0033, Japan

[d]Elements Strategy Initiative for Catalysts and Batteries (ESICB), Kyoto University, Katsura, Kyoto 615-8520, Japan

[e]RIKEN SPring-8 Center, 1-1-1 Kouto, Sayo-cho, Sayo-gun, Hyogo 679-5148, Japan

[f]Department of Chemistry, Faculty of Science, Hokkaido University, Nishi 8, Kita 10, Kita-ku, Sapporo 060-0810, Japan

Contents

1. Experimental details

Preparation: To prepare the AuCu nanoalloy (NA), 0.25 mmol of $Cu(OAc)_2$ and 0.555g of poly[vinyl-2-pyrrolidone] were dissolved into an aqueous mixture of 2-ethoxyethanol (90 vol.%), and 8.33 ml aqueous solution of $HAuCl_4$ (30mM) was then mixed into the $Cu(OAc)_2$ solution at 273 K. The solution was maintained at this temperature, while 10 ml aqueous solution of $NaBH_4$ was added. Just after the addition of $NaBH_4$, the color of the solution became a black-brown color, indicating reduction of the metal salts. This reaction solution was then stirred continuously for 2 h. A black precipitate was obtained after adding a mixed solvent of acetone and diethyl ether (3:2) and washing with water using a filtration technique. The final product was dried and kept in a desiccator. The synthetic procedure for the preparation of Au nanoparticles was almost similar to that of the AuCu NA. 60 ml aqueous solution of $HAuCl_4$ (30mM) was used as a metal precursor.

Characterization: Transmission electron microscope (TEM) images of the sample were taken with a JEM-2100F (JEOL) instrument operated at 200 kV. Elemental analysis was conducted using inductively coupled plasma atomic emission spectroscopy (ICP-AES) with an ICPE-9000 spectrometer (Shimazu). X-ray photoelectron spectra were recorded with a JPC-9010MC (JEOL) using non-monochromatized MgKa radiation at a power of 200 W. Binding energy was corrected by referring to the binding energies of poly[vinyl-2-pyrrolidone][1,2]. To identify the prepared AuCu NA before the synchrotron X-ray study, X-ray diffraction (XRD) patterns were collected with D8 ADVANCE diffractometer using Cu Kα radiation (Bruker). In-situ synchrotron XRD measurements under vacuum and hydrogen were carried out with a Debye-Scherrer camera installed on the RIKEN Materials Science Beamline BL44B2 at SPring-8. An incident wavelength of 0.58 Å was used to reduce absorption effects on the diffraction intensities. To record the fast disorder-order phase transformation, a homemade gas line system (developed in house) equipped with an electromagnetic valve near the sample position was synchronized with the sample temperature controller and an X-ray flat panel sensor (C10158DK-11, Hamamatsu Photonics K.K., Japan). The frame rate of the flat panel sensor was fixed at 3 frames/s, which corresponds to approximately 0.333

s/frame for the X-ray exposure time. The starting point for each measurement was assigned to the opening time of the X-ray shutter on the diffractometer. For the measurements under hydrogen, we opened the electromagnetic valve within 1 s after opening of the X-ray shutter. A schematic of the system layout is shown in Figure S2. For a more detailed structural characterization, an imaging plate (IP), which has a wider dynamic range, was employed for measurements using a wavelength of 0.579865(4) Å. To apply the Rietveld method to the IP data, X-ray exposure time was set to 5 minutes at the sacrifice of time resolution. Lab-based XRD experiment was performed using D8 ADVNCE diffractometer (Bruker) equipped with an X-ray tube (Cu Ka) and an 1-dimentional detector (LYNXEYE^{TM}, Bruker) which can suppress the influence of fluorescence radiated from samples. Rietveld profile analyses for the XRD patterns were carried out using Topas4 software provided by Bruker. In the analysis, the alloy compositions in the $L1_0$ and fcc phase were assumed to be $Au_{50}Cu_{50}$ and $Au_{55}Cu_{45}$, respectively, based on the ICP-AES result. The other parameters, such as lattice constants, crystal sizes, site occupancies by an element and mass ratios of $L1_0$ and fcc phases were determined by the refinement. Hydrogen pressure-composition isotherms were obtained with a BEL-HP automatic gas absorption system (BEL JAPAN). As a pretreatment, the AuCu NAs were evacuated at room temperature for 2 days, at 373 K for a day and at 453 K for a few hours. ^{2}H wide-line and ^{2}H magic-angle-spinning (MAS) NMR experiments were performed at 46.1 MHz using an Apollo NMR spectrometer (Techmag). Wide-line NMR signals were accumulated 10,000-40,000 times by employing a quadrupole echo sequence with a 500-ns dwell time and ~4-s repetition time. The MAS NMR spectra were obtained using a 4.0-mm rotor with a 90°-τ-180° echo synchronized to magic angle rotation (τ = 1/7 kHz) sequence.

References

1 B. Choi, H. Yoon, I.-S. Park, J. Jang, Y.-E. Sung, *Carbon,* 2007, **45**, 2496.

2 G. Beamson, D. Briggs, *High Resolution XPS of Organic Polymers: the Scienta ESCA300 Database*, 1992

2. TEM images of AuCu NAs before and after the hydrogen exposure treatment

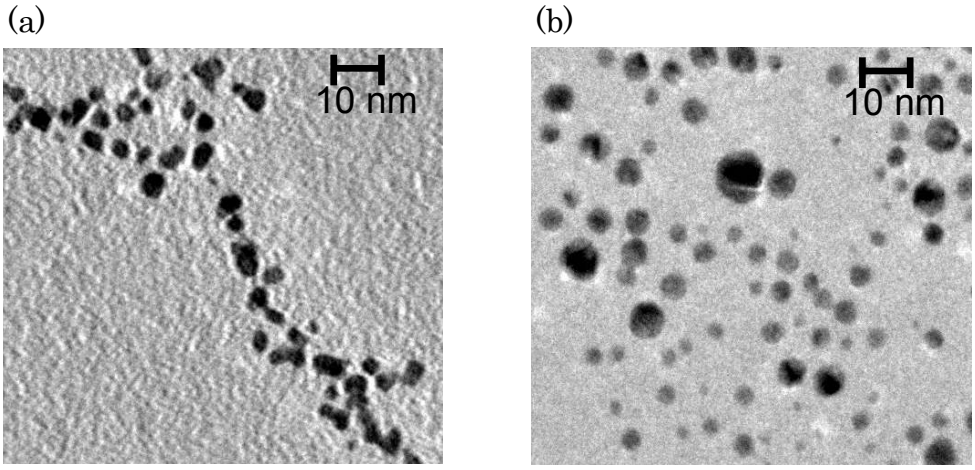

Figure S1. TEM images of AuCu NAs (a) as synthesized and (b) after exposure to 100 kPa of hydrogen at 453 K for 120 min.

3. X-ray photoelectron spectra of AuCu NAs and Au nanoparticles

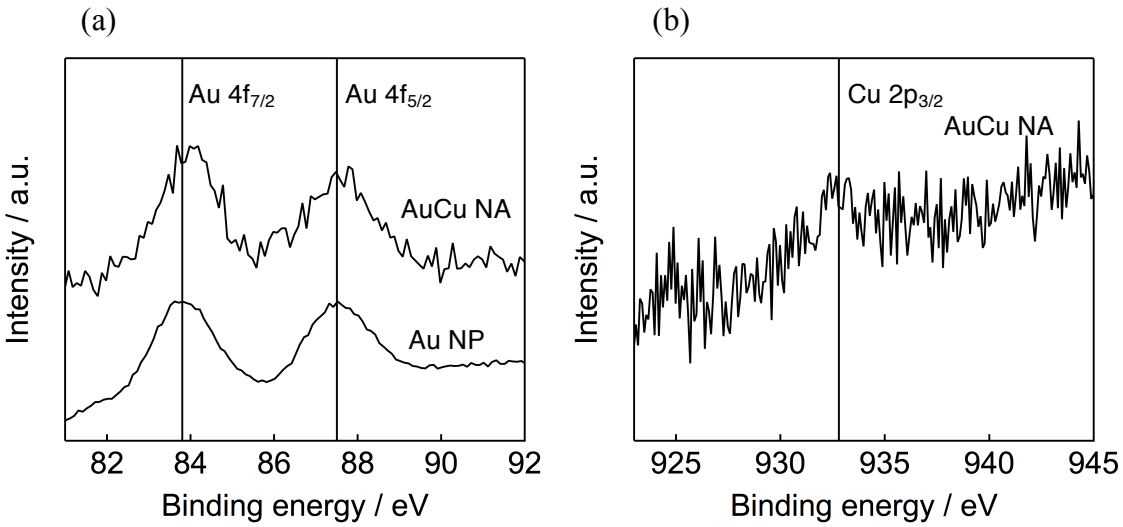

Figure S2. (a) Au $4f_{7/2,5/2}$ X-ray photoelectron spectra of AuCu NAs and Au nanoparticles (NPs) and (b) Cu $2p_{3/2}$ X-ray photoelectron spectrum of AuCu NAs. Binding energies in corresponding metals are indicated by solid lines.

4. Structural parameters of the $L1_0$-AuCu NA determined by Rietveld analysis

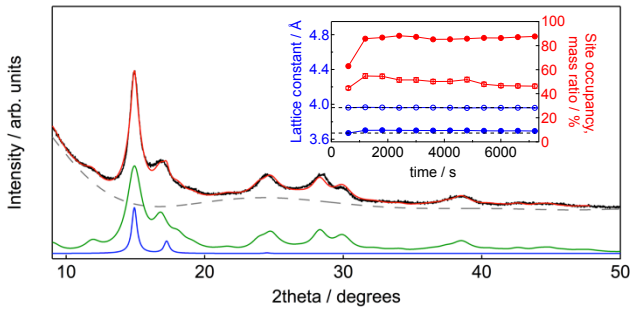

Figure S3. The Rietveld profile (red) calculated for the XRD pattern of the AuCu NA measured at 453 K after exposure to hydrogen for 7200 s, assuming $L1_0$ (green), fcc structures (blue) and background (broken). Structural parameters of the $L1_0$ phase forming under hydrogen at 453 K, such as lattice constants (left) ; a(◯) and c(●), the site occupancies (right, ●) and mass ratios of $L1_0$-phase (right, ◯) in the NA, are plotted in inset.

5. XRD equipment installed on the RIKEN Materials Science Beamline BL44B2 at SPring-8

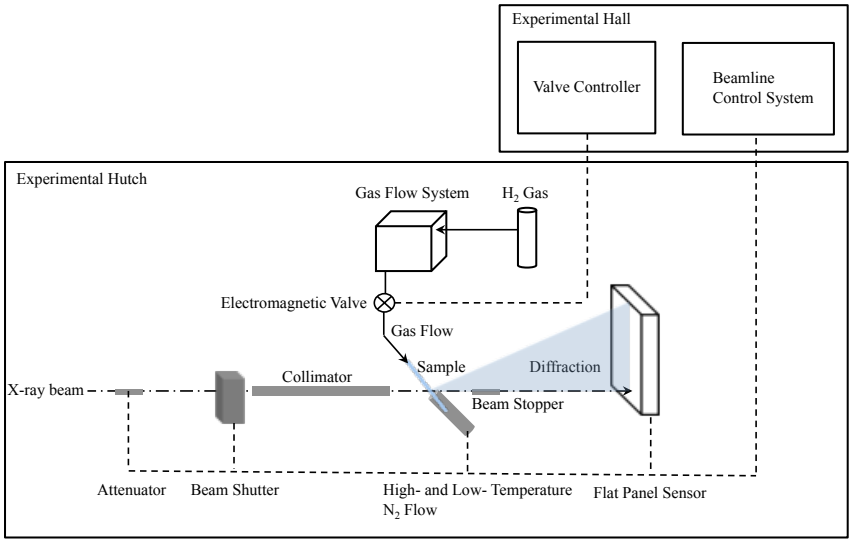

Figure S4. Schematic of the system used for the in situ time-resolved XRD measurements. The system synchronizes the hydrogen pressure control, sample temperature control and X-ray exposure systems.

6. XRD patterns of the AuCu NA obtained using a flat panel sensor

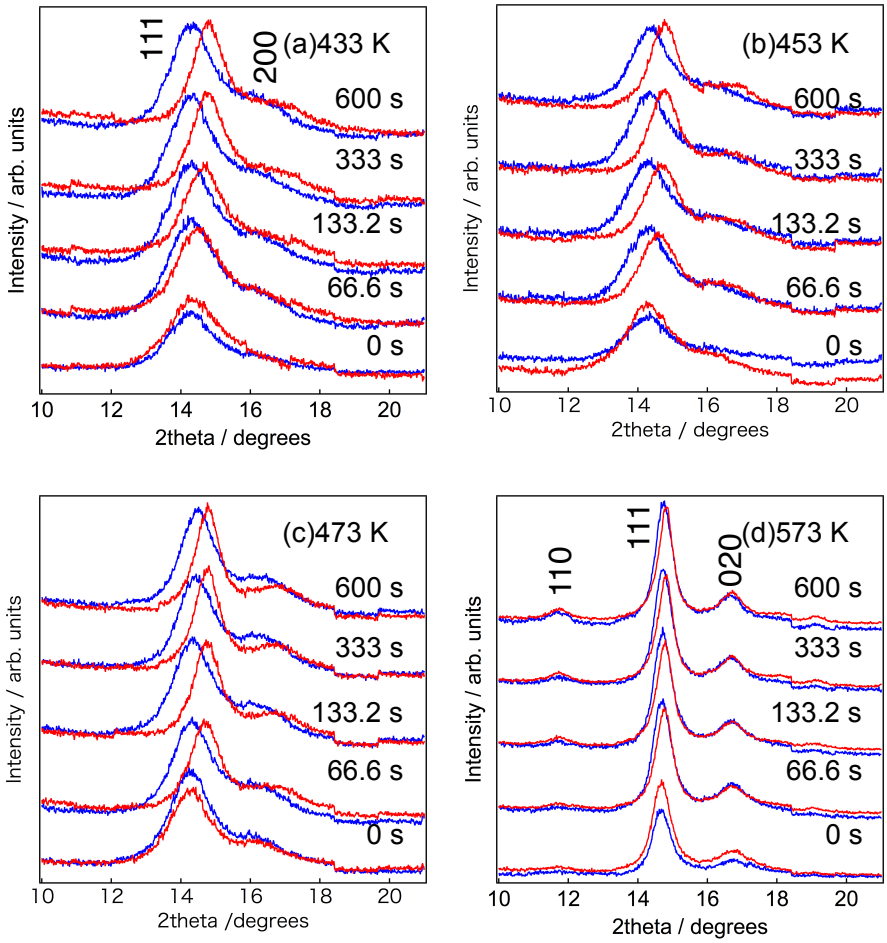

Figure S5. XRD patterns of AuCu NAs obtained under vacuum (blue) and under 100 kPa of hydrogen (red) measured at (a) 433, (b) 453, (c) 473 and (d) 573 K. Each pattern was calculated from one frame recorded on the flat panel. The elapsed time after the X-ray shutter has opened is given on the right.

7. ^{2}H wide-line and ^{2}H magic-angle-spinning (MAS) NMR spectra

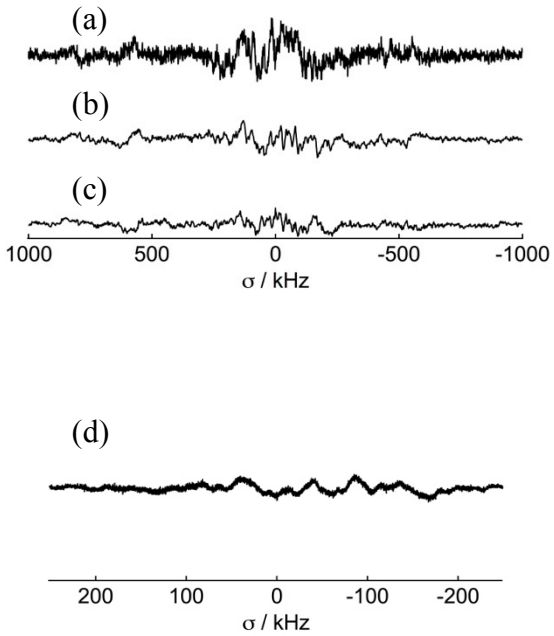

Figure S6. ^{2}H wide-line spectra of (a) the AuCu NA evacuated after exposure to deuterium at 453 K for 2 h and (b) PVP evacuated after exposure to deuterium at 453 K for 2 h. (c) The background signal of ^{2}H wide-line NMR measurements. (d) ^{2}H MAS NMR spectrum of the AuCu NA after exposure to deuterium at 453 K for 2 h.